Journal of Alloys and Compounds 509 (2011) 9055–9059

Contents lists available at ScienceDirect

Journal of Alloys and Compounds

journal homepage: www.elsevier.com/locate/jallcom

Dehydrogenation kinetics of $2LiBH_4 + MgH_2$ enhanced by hydrogen back pressure and a $CuCl_2$ catalyst

Ying Jiang, Bin Hong Liu*

Dept. of Materials Sci. & Eng., Zhejiang University, Hangzhou 310027, Zhejiang, China

ARTICLE INFO

Article history:
Received 30 March 2011
Received in revised form 22 May 2011
Accepted 23 May 2011
Available online 6 July 2011

Keywords:
Reactive hydride composite
Dehydrogenation
Kinetics
Hydrogen back pressure
Nucleation

ABSTRACT

In this work, the dehydrogenation kinetics of the $2LiBH_4 + MgH_2$ composite under different hydrogen back pressures was studied. The applied hydrogen back pressure significantly influenced the hydrogen release rate of the uncatalyzed composite. Higher hydrogen pressures enhanced the nucleation of MgB_2, resulting in better dehydrogenation kinetics and cycle stability. The composite with a $CuCl_2$ catalyst demonstrated significantly improved dehydrogenation kinetics because the nucleation of MgB_2 was promoted by heterogeneous nuclei. However, similar effects of hydrogen back pressure on dehydrogenation kinetics were also observed for the $CuCl_2$-catalyzed composite. The extraordinary results suggest that hydrogen back pressure plays an indispensable role in the formation of MgB_2, which determines not only the reaction pathway but also the kinetics of dehydrogenation for the $2LiBH_4 + MgH_2$ composite.

1. Introduction

$LiBH_4$, a chemical hydride containing 18.4 wt.% hydrogen, has recently attracted considerable attention as a potential hydrogen storage medium [1,2]. However, its reversible hydrogen storage requires high temperatures and/or pressures.

$$LiBH_4 \leftrightarrow LiH + B + 3/2H_2 \quad (1)$$

In the above reaction, $LiBH_4$ releases 13.8 wt.% hydrogen at temperatures above 400 °C. Rehydrogenation has to be performed at temperatures much higher, around 600 °C, and under 15 MPa H_2 [3]. To enhance the hydrogen storage performance of $LiBH_4$ under moderate conditions, extensive effort has been focused on the destabilization of $LiBH_4$ using various additives, such as metals, metal hydrides, oxides, halides, and carbon materials [4–12]. A reactive hydride composite, $2LiBH_4 + MgH_2$, developed by Vajo et al. [4] exhibited promising hydrogen storage properties in terms of its reduced thermal stability, high hydrogen capacity (11.5 wt.%), and good reversibility in the following reaction:

$$2LiBH_4 + MgH_2 \leftrightarrow 2LiH + MgB_2 + 4H_2 \quad (2)$$

Compared with pure $LiBH_4$, the $2LiBH_4 + MgH_2$ composite demonstrated significantly improved hydrogen storage properties. Shaw et al. [13–15] have reported that solid state hydriding and dehydriding below the melting temperature of $LiBH_4$ (~280 °C) were achieved through high-energy ball milling. Further research efforts are needed to reduce hydriding and deydriding temperatures to near ambient temperature.

In practice, dehydrogenation of the $2LiBH_4 + MgH_2$ composite does not proceed through the direct reaction between $LiBH_4$ and MgH_2. Instead, it is accomplished through two steps: Initially, MgH_2 desorbs hydrogen to form Mg and then Mg reacts with $LiBH_4$ to yield LiH and MgB_2. However, MgB_2 is difficult to form, which impedes the subsequent dehydrogenation process [16]. Catalysts such as $TiCl_3$ are usually used to enhance the hydriding–dehydriding kinetics of $2LiBH_4 + MgH_2$ [4,17,18]. Other additives, including Al, Zr, V, Nb, Pd, C, or their compounds, have also been used for $2LiBH_4 + MgH_2$ [19–25]. Enhancements of dehydriding kinetics through these catalytic additives are usually ascribed to the formation of some transition metal borides, such as TiB_2 and ZrB_2, which function as heterogeneous nuclei for MgB_2 formation. The hydrogen back pressure applied in the reactor is an important factor in deciding the reaction pathway of dehydrogenation for $2LiBH_4 + MgH_2$ [4,17]. Under low hydrogen pressures, $LiBH_4$ decomposes independently into LiH and amorphous boron without reacting with Mg to form MgB_2. As a result, the reaction becomes quite irreversible. At least a hydrogen back pressure of 3 bar at 450 °C is reportedly necessary to suppress the independent decomposition of $LiBH_4$ and to obtain MgB_2 for the reversible hydrogen storage reaction. However, the effects of hydrogen pressure on dehydrogenation of $2LiBH_4 + MgH_2$ have not yet been clarified fully, and the mechanism remains unclear. Therefore, in this study, a detailed investigation was carried out to reveal how

* Corresponding author. Tel.: +86 571 87951770; fax: +86 571 87951770.
E-mail address: liubh@zju.edu.cn (B.H. Liu).

0925-8388/$ – see front matter © 2011 Elsevier B.V. All rights reserved.
doi:10.1016/j.jallcom.2011.05.087

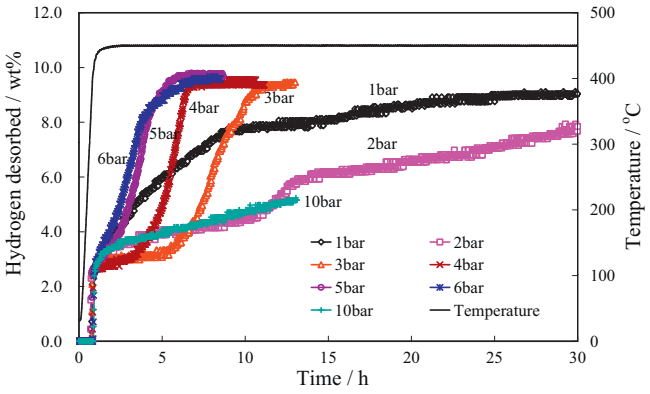

Fig. 1. Dehydrogenation kinetics of $2LiBH_4 + MgH_2$ at 450 °C under different hydrogen back pressures.

the hydrogen back pressure influences the dehydrogenation reaction of $2LiBH_4 + MgH_2$, with emphasis on its effects on dehydriding kinetics. The use of $CuCl_2$ as a catalytic additive in $2LiBH_4 + MgH_2$ is also presented. The results may facilitate the understanding of the hydrogen storage mechanisms of $2LiBH_4 + MgH_2$, as well as other $LiBH_4$-based reactive composites. This study, although was conducted at temperatures higher than the melting point of $LiBH_4$, can hopefully shed some light on the selection of catalysts and operational conditions for solid state hydriding and dehydriding.

2. Experimental

$LiBH_4$ (95% purity, Acros) was used as received without further purification. MgH_2 was prepared by hydriding Mg powder (100–200 mesh) at 400 °C under 30 bar for 12 h. Anhydrous $CuCl_2$ was prepared by dehydrating $CuCl_2 \cdot 2H_2O$ (99%) at 130 °C under a vacuum for 2 h. Samples of $2LiBH_4 + MgH_2$ with and without catalysts were ball-milled in a planetary mill at 500 rpm for 16 h. The volume of the stainless steel vessel for ball milling was 100 mL. The ball to sample weight ratio was 213:1. No detectable contaminations from the vessel and balls were found for the ball-milled samples.

The dehydrogenation and hydrogenation properties of the composite were examined using a Sieverts apparatus. During the dehydrogenation experiments, the reactor was first heated at a rate of 10 °C min^{-1} to 450 °C, after which the temperature was maintained under a nearly fixed hydrogen back pressure. The amount of hydrogen desorbed was determined according to the pressure rise in the system. The hydrogen desorbed in wt.% was determined relative to $2LiBH_4 + MgH_2$ without including the weight of the catalysts. The hydrogenation was performed by holding the dehydrogenated sample at 350 °C under 40 bar for 16 h. All sample handling was performed in a glove box under a high-purity argon atmosphere to prevent air contamination. The O_2 and H_2O levels in the glove box were kept below 1 ppm.

X-ray diffraction (XRD) measurements were performed on a PANalytical X'Pert PRO diffractometer using CuK_α radiation. A sample stand was specially prepared to keep the samples from atmospheric exposure during sample transfers and XRD measurements. The sample window was covered with a layer of transparent plastic film that demonstrated no specific peaks in the XRD patterns.

3. Results

3.1. Effects of hydrogen back pressure on dehydriding kinetics of the uncatalyzed composite

Although there have been several studies on the effects of hydrogen back pressure on dehydrogenation of $2LiBH_4 + MgH_2$ [17,25,26], most of these focused on identifying the reaction products and determining the reaction pathway through various instrumental analyses, such as in situ X-ray diffraction. However, little is known of the effects of hydrogen back pressure on the dehydrogenation kinetics of $2LiBH_4 + MgH_2$. Hence, this paper studies the dehydriding kinetics of uncatalyzed $2LiBH_4 + MgH_2$ under different hydrogen back pressures. As shown in Fig. 1, the behavior of hydrogen release changed remarkably under different hydrogen back pressures. Initially, the rate of dehydrogenation decreased

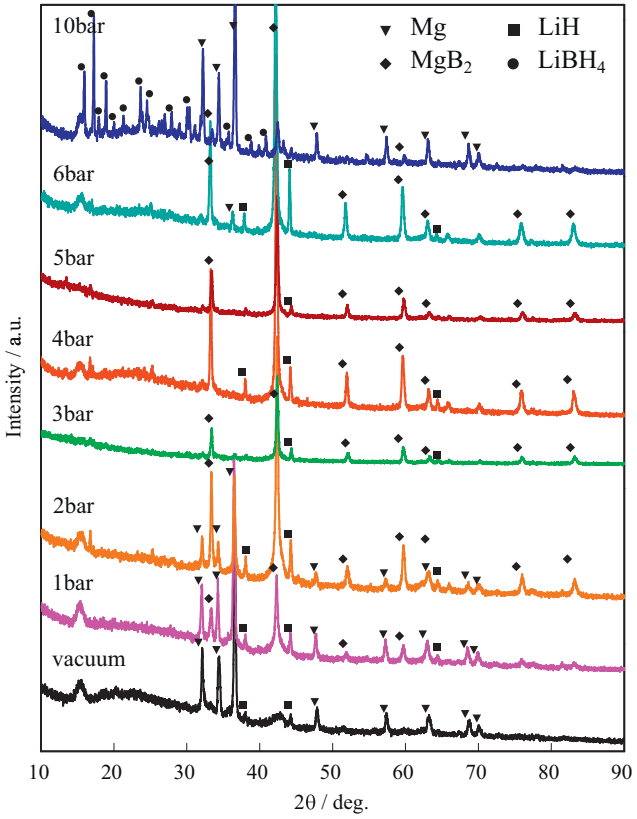

Fig. 2. XRD patterns of the $2LiBH_4 + MgH_2$ composite after dehydrogenation at 450 °C under different hydrogen back pressures.

when the back pressure was increased from 1 bar to 2 bar. A long incubation period was observed for dehydrogenation carried out under 3 bar. When the hydrogen back pressure was further increased, the incubation period shortened and the dehydrogenation kinetics was enhanced. However, dehydrogenation became incomplete when the pressure was increased up to 10 bar.

The products of dehydrogenation under different back pressures were determined based on the XRD patterns shown in Fig. 2. Large amounts of Mg were detected in the samples dehydrogenated under hydrogen pressures below 3 bar. In particular, no MgB_2 was present in the composite dehydrogenated under a dynamic vacuum. The amount of Mg decreased and that of MgB_2 increased with increasing hydrogen back pressure until no Mg was detected in the samples dehydrogenated under 3–5 bar. Mg reappeared in the samples when the back pressure was increased to 6 bar. Large portions of unreacted $LiBH_4$ and Mg were also detected in the sample dehydrogenated under a hydrogen pressure of 10 bar.

Based on the kinetic observations and XRD results shown in Figs. 1 and 2, the dehydrdogenation of the uncatalyzed $2LiBH_4 + MgH_2$ composites could be analyzed as follows. Initially, all the dehydrogenation curves demonstrated a rapid release of about 2.6–2.9 wt.% hydrogen. This amount of hydrogen corresponded to hydrogen desorption of MgH_2 in the composites. Therefore, all the dehydrogenation procedures began with rapid hydrogen desorption from MgH_2 to form metallic Mg. Subsequent hydrogen desorption was then influenced significantly by the applied hydrogen back pressure. Hydrogen desorption under a dynamic vacuum did not produce MgB_2, indicating that $LiBH_4$ decomposed independently into LiH and amorphous boron. A C-type dehydrogenation curve and only a small amount of MgB_2 were obtained by dehydriding under 1 bar, suggesting that hydrogen desorption proceeded mainly through independent $LiBH_4$ decomposition. Under a hydrogen pressure of 2 bar, the rate of hydrogen

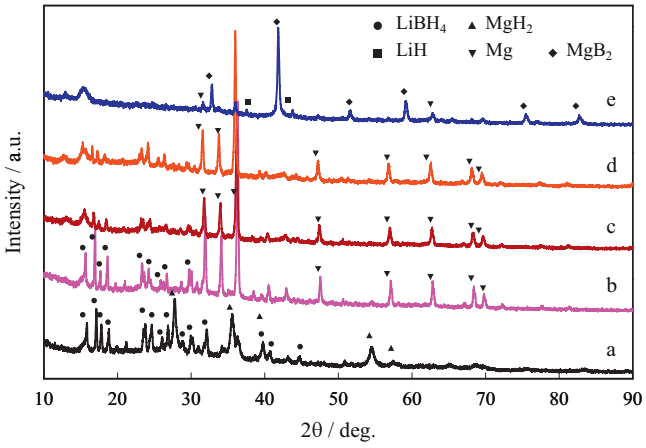

Fig. 3. XRD patterns of the initial $2LiBH_4 + MgH_2$ at different dehydrogenation stages. (a) After ball milling; (b) maintained at 450 °C under 3 bar H_2 for 1 h; (c) for 3 h; (d) for 5 h; and (e) for 9 h.

desorption decreased compared with that under 1 bar, whereas the amount of MgB_2 largely increased in the dehydrogenated sample. These results suggest that the independent decomposition of $LiBH_4$ was suppressed, whereas its reaction with Mg increased. Under a back pressure of 3 bar, a long incubation period of 5 h was observed prior to a relatively rapid hydrogen release. Based on the XRD results shown in Fig. 2, dehydrogenation under this condition appears to proceed mainly through the reaction between Mg and $LiBH_4$. According to the XRD patterns shown in Fig. 3, there was no MgB_2 present during the incubation period. The long incubation period was thus ascribed to the nucleation of MgB_2. The incubation time decreased unusually when the hydrogen pressure was further increased. Dehydrogenation under 5–6 bar demonstrated the best kinetics because the reaction became incomplete when the pressure was increased up to 10 bar. This is because the hydrogen pressure at this time approached the equilibrium pressure of the dehydrogenation reaction.

Fig. 4 shows the dehydrogenation behavior of the uncatalyzed $2LiBH_4 + MgH_2$ upon cycling performed by dehydriding the composite at 450 °C under 5 bar H_2 and then hydriding it at 350 °C under 40 bar H_2 for 16 h. The composite demonstrated a reversible capacity of 9.7 wt.% under these conditions. The dehydriding kinetics gradually improved within four cycles. Moreover, almost no capacity loss over the cycling was observed. The composite demonstrated poor cycle stability when it was dehydrogenated under hydrogen back pressures below 3 bar.

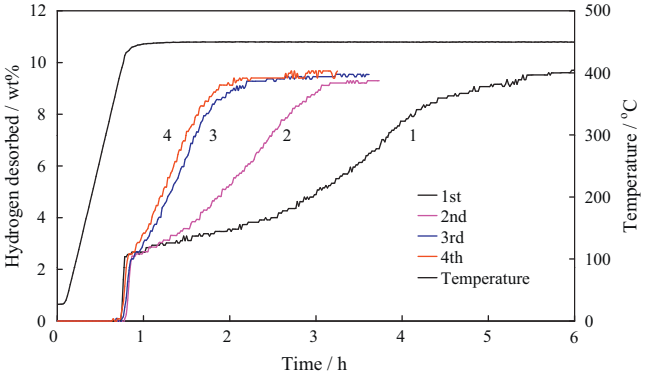

Fig. 4. Dehydrogenation kinetics of $2LiBH_4 + MgH_2$ at 450 °C under a hydrogen back pressure of 5 bar for four cycles (hydrogenation: 350 °C, 40 bar H_2, 16 h).

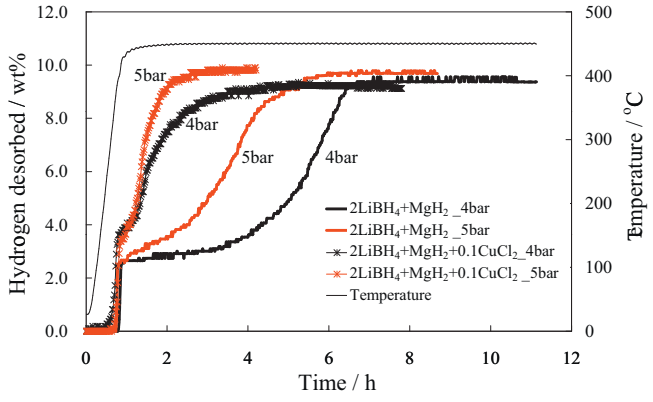

Fig. 5. Dehydriding kinetics of the pure and $CuCl_2$-added $2LiBH_4 + MgH_2$ composites at 450 °C under 4 bar or 5 bar H_2.

3.2. Catalytic effects of $CuCl_2$ in the composites

In this study, $CuCl_2$ was used as a catalytic additive in $2LiBH_4 + MgH_2$ to improve its hydrogen storage properties and determine whether or not a non-boride forming additive could promote dehydrogenation of $2LiBH_4 + MgH_2$ effectively. As shown in Fig. 5, the $CuCl_2$-added composite demonstrated significantly improved dehydrogenation kinetics compared with the uncatalyzed composite mainly because the incubation time significantly shortened after $CuCl_2$ addition. The XRD analysis results shown in Fig. 6 demonstrate that LiCl, Mg_2Cu, and $MgCu_2$ were also formed. Although no boride of copper was produced, the nucleation of MgB_2 was apparently promoted due to the $CuCl_2$ addition. Based on the XRD results shown in Fig. 6, $CuCl_2$ in the composite appears to react with some portions of $LiBH_4$ to produce LiCl and metallic Cu. The

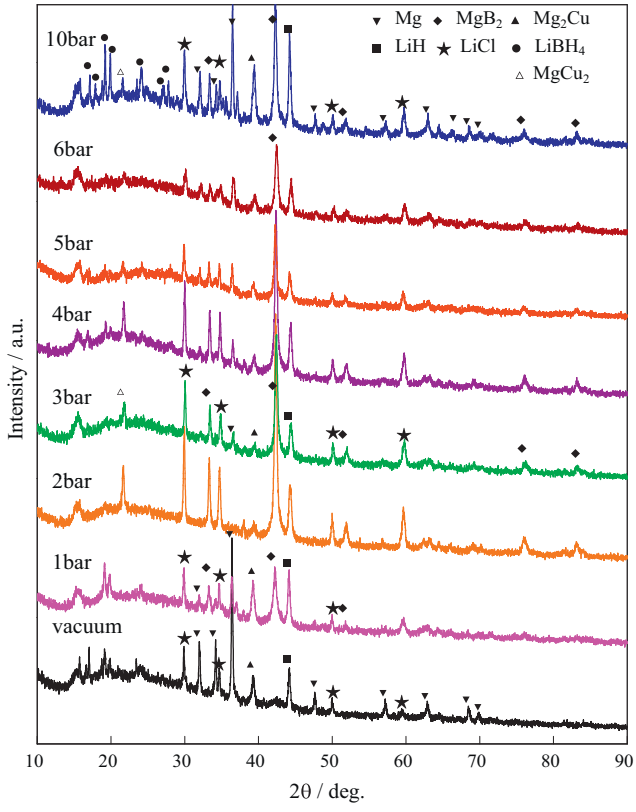

Fig. 6. XRD patterns of $2LiBH_4 + MgH_2 + 0.1CuCl_2$ after dehydrogenation at 450 °C under different hydrogen back pressures.

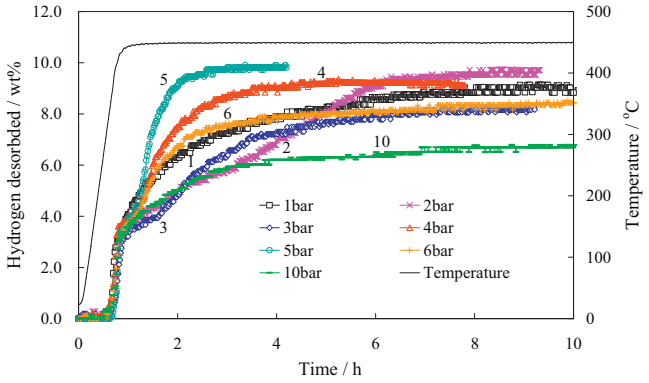

Fig. 7. Dehydrogenation kinetics of $2LiBH_4 + MgH_2 + 0.1CuCl_2$ at 450 °C under different hydrogen back pressures.

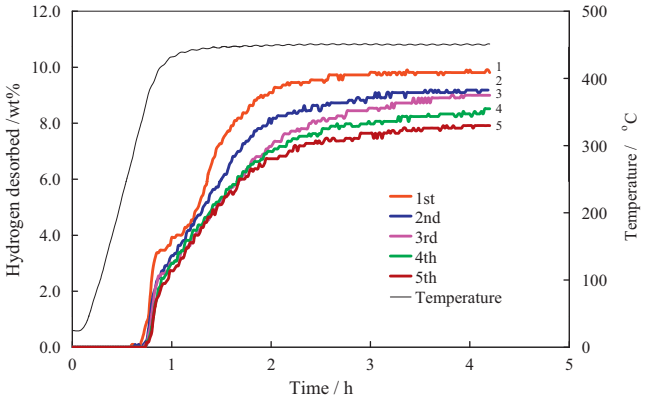

Fig. 8. Dehydrogenation kinetics of $2LiBH_4 + MgH_2 + 0.1CuCl_2$ at 450 °C under a hydrogen back pressure of 5 bar for five cycles (hydrogenation conditions: 350 °C, 40 bar H_2, 16 h).

latter then reacted with MgH_2 to form Mg_2Cu and $MgCu_2$, which might function as heterogeneous nuclei for MgB_2 formation.

3.3. Effects of hydrogen back pressure in the presence of $CuCl_2$ catalyst

Although the composite with the $CuCl_2$ catalyst demonstrated significantly improved dehydrogenation kinetics, its dehydriding behavior was still influenced by the applied hydrogen back pressure. As shown in Fig. 7, dehydrogenation of $2LiBH_4 + MgH_2 + 0.1CuCl_2$ under hydrogen pressures varying from 1 bar to 10 bar demonstrated tendencies similar to those of the uncatalyzed composite. As the back pressure was increased, the rate of hydrogen release first decreased and then increased with a turn at 3 bar. The best kinetics was achieved when dehydrogenation was carried out under 5 bar. When the hydrogen pressure was over 6 bar, the amount of hydrogen desorbed gradually decreased with increasing back pressure.

The results of XRD analysis shown in Fig. 6 also indicate that no MgB_2 was obtained when dehydrogenation of $2LiBH_4 + MgH_2 + 0.1CuCl_2$ was carried out under a dynamic vacuum, suggesting that a hydrogen pressure is requisite for MgB_2 formation even in the presence of a catalyst. The peaks from Mg gradually weakened, whereas those from MgB_2 strengthened as the hydrogen back pressure increased, indicating that most of the Mg was transformed into MgB_2. When the back pressure was increased to 10 bar, some Mg and $LiBH_4$ remained unreacted, suggesting that the back pressure approached the equilibrium pressure of the dehydrogenation reaction.

Fig. 8 reveals the cycling stability of the $CuCl_2$-added composite. The composite demonstrated stable dehydriding kinetics over five dehydriding–rehydriding cycles, but showed gradual decreases in hydrogen storage capacity during cycling. The XRD analysis of the cycled composite could not provide clues to explain the capacity loss, thus further investigation is necessary to determine the reason.

3.4. Kinetic analysis of the dehydrogenation process

As shown above, the formation of MgB_2 during dehydrogenation of the $2LiBH_4 + MgH_2$ composite proceeds via a typical nucleation-growth process. For a nucleation-growth mechanism, the kinetic equation of Johnson–Mehl–Avrami can be applied [27].

$$f = 1 - \exp[-k(t-\tau)^n] \quad (3)$$

where f is the volumetric fraction of the reaction at time t, τ is the incubation time, k is the rate constant, and n is the Avrami exponent. The values of k and n can be obtained by plotting $\ln[-\ln(1-x)]$

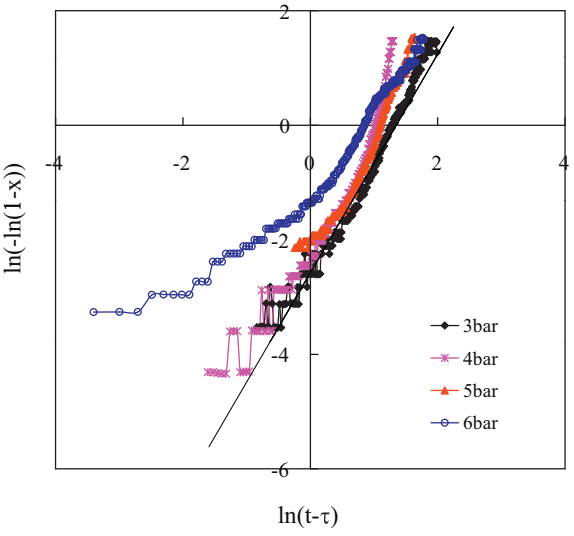

Fig. 9. $\ln(-\ln(1-x))$ vs. $\ln(t-\tau)$ for the Mg + $LiBH_4$ reaction under different H_2 back pressures (drawn from the dehydrogenation curves shown in Fig. 1).

versus $\ln(t-\tau)$, as shown in Fig. 9. Table 1 lists the values of k and n under different hydrogen pressures with and without the $CuCl_2$ addition. As can be seen in Table 1, the Avrami exponents obtained are larger than 1.5 for the uncatalyzed composite and smaller than 1.5 for the $CuCl_2$-catalyzed composite. According to Ref. [27], a value of n larger than 1.5 corresponds to a kinetics of transformation with continual nucleation, whereas a value smaller than 1.5 corresponds to a kinetics via growth of initially formed nuclei. Accordingly, MgB_2 was formed in the uncatalyzed composite through continual nucleation and hydrogen back pressure

Table 1
Calculated Avrami exponent n and rate constant k for MgB_2 transformation.

	n	k
$2LiBH_4 + MgH_2$		
H_2 back pressure		
3 bar	2.1	0.11
4 bar	2.4	0.09
5 bar	2.6	0.13
6 bar	1.7	0.26
$2LiBH_4 + MgH_2 + 0.1CuCl_2$		
H_2 back pressure		
3 bar	1.2	0.37
4 bar	1.1	0.93
5 bar	1.4	1.84

increased the rate of nucleation, whereas the transformation of MgB_2 in the $CuCl_2$-catalyzed composite was mainly via growth of initially formed nuclei. This agrees well with the practical situation in which initially formed Mg_2Cu or $MgCu_2$ may act as heterogeneous nuclei for MgB_2 formation.

4. Discussion

The results shown above reveal that dehydrogenation of $2LiBH_4 + MgH_2$ composite is highly dependent on the applied hydrogen back pressure. The back pressure not only determined the reaction pathway of dehydrogenation, but also enhanced the dehydriding kinetics by promoting the nucleation of MgB_2. The higher the hydrogen pressure, the shorter the incubation period of MgB_2 nucleation became. Even in the presence of the $CuCl_2$ catalyst, H_2 back pressure demonstrated obvious effects on the reaction pathway and kinetics of dehydrogenation. This behavior is extraordinary for a hydrogen-releasing reaction because a high back pressure means a low driving force for dehydrogenation. These uncommon results are largely related to the formation of MgB_2. Here, hydrogen back pressure is required for two reasons: first, sufficient back pressure is required to suppress the independent decomposition of $LiBH_4$ into LiH and B; second, higher H_2 pressure can enhance the formation of MgB_2 nuclei.

It is still unclear how a high H_2 pressure promotes the nucleation of MgB_2. Nakagawa et al. [18] suggested that hydrogen could introduce some defects into the composite and reduce the activation barrier. Shim et al. [26] proposed two mechanisms for the effects shown by hydrogen back pressure. One is that hydrogen pressure would prevent the formation of amorphous boron or $Li_2B_{12}H_{12}$, which may cover the solid particles (Mg in this work) and impede the contact between solid particles and liquid $LiBH_4$. The other mechanism is that hydrogen back pressure may improve the wetting between liquid $LiBH_4$ and solid particles. However, these mechanisms cannot explain the indispensable role of hydrogen in MgB_2 nucleation even in the presence of catalytic additives.

MgB_2 has a layered structure in which layers of Mg and B are distributed alternately. During dehydrogenation of the composite, MgB_2 is formed in an environment with three phases: a solid phase (Mg), a liquid phase ($LiBH_4$), and a gas phase (H_2). A possible mechanism for the dependence on hydrogen back pressure is that MgB_2 is formed at the interfaces of the three phases. Another possibility is that an MgH_x solid solution is formed under high hydrogen pressures, which may favor the formation of MgB_2. Further investigations are required to verify these assumptions.

5. Conclusions

In this work, the effects of hydrogen back pressure on dehydrogenation of $2LiBH_4 + MgH_2$ were systematically examined. Hydrogen desorption of the uncatalyzed composite was influenced remarkably by the applied back pressure. The dehydrogenation rate first decreased and then increased as hydrogen back pressure was increased. Hydrogen back pressure not only determined the reaction pathway of dehydrogenation, but also promoted the nucleation of MgB_2 and thus improved the dehydrogenation kinetics and cycle stability of the composite. The composite with the $CuCl_2$ catalyst demonstrated significantly improved dehydrogenation kinetics due to the enhanced nucleation of MgB_2. Hydrogen back pressure revealed similar effects during dehydrogenation of the $CuCl_2$-catalyzed composite. The results obtained strongly suggest that hydrogen plays an indispensable role in the formation of MgB_2.

Acknowledgements

This work is financially supported by the National Natural Science Foundation under No. 50971114 as well as the Hi-tech projects of Zhejiang Province under No. 2009C21011.

References

[1] A. Züttel, P. Wenger, S. Rentsch, P. Sudan, Ph. Mauron, Ch. Emmenegger, J. Power Sources 118 (2003) 1–7.
[2] S. Orimo, Y. Nakamori, J.R. Eliseo, A. Züttel, C.M. Jensen, Chem. Rev. 107 (2007) 4111–4132.
[3] P. Mauron, F. Buchter, O. Friedrichs, A. Remhof, M. Bielmann, C.N. Zwicky, A. Züttel, J. Phys. Chem. B 112 (2008) 906–910.
[4] J.J. Vajo, S.L. Skeith, F. Mertens, J. Phys. Chem. B 109 (2005) 3719–3722.
[5] J.J. Vajo, G.L. Olson, Scripta Mater. 56 (2007) 829–834.
[6] J. Yang, A. Sudik, C. Wolverton, J. Phys. Chem. C 111 (2007) 19134–19140.
[7] X.D. Kang, P. Wang, L.P. Ma, H.M. Cheng, Appl. Phys. A 89 (2007) 963–966.
[8] A.F. Gross, J.J. Vajo, S.L. Van Atta, G.L. Olson, J. Phys. Chem. C 112 (2008) 5651–5657.
[9] X.B. Yu, Z. Wu, Q.R. Chen, Z.L. Li, B.C. Weng, T.S. Huang, Appl. Phys. Lett. 90 (2007) 034106–34113.
[10] M. Au, A. Jurgensen, J. Phys. Chem. B 110 (2006) 7062–7067.
[11] M. Au, A. Jurgensen, K. Zeigler, J. Phys. Chem. B 110 (2006) 26482–26487.
[12] S.A. Jin, Y.S. Lee, J.H. Shim, Y.W. Cho, J. Phys. Chem. C 112 (2008) 9520–9524.
[13] X. Wan, T. Markmaitree, W. Osborn, L.L. Shaw, J. Phys. Chem. C 112 (2008) 18232–18243.
[14] K. Crosby, L.L. Shaw, Int. J. Hydrogen Energy 35 (2010) 7519–7529.
[15] L.L. Shaw, Wan.XJ.Z. Hu, J.H. Kwak, Z. Yang, J. Phys. Chem. C 114 (2010) 8089–8098.
[16] U. Bösenberg, S. Doppiu, L. Mosegaard, G. Barhordarian, N. Eigen, A. Borgschulte, T.R. Jensen, Y. Cerenius, O. Gutfleisch, T. Klassen, M. Dornheim, R. Bormann, Acta Mater. 55 (2007) 3951–5958.
[17] F.E. Pinkerton, M.S. Meyer, G.P. Meisner, M.P. Balogh, J.J. Vajo, J. Phys. Chem. C 111 (2007) 12881–12885.
[18] T. Nakagawa, T. Ishikawa, N. Hanada, Y. Kojima, H. Fujii, J. Alloys Compd. 446–447 (2007) 306–309.
[19] E. Deprez, A. Justro, T.C. Rojas, C. Lopez-Cartes, C.B. Bonatto Minella, U. Bösenberg, M. Dornheim, R. Bormann, A. Fernandez, Acta Mater. 58 (2010) 5683–5694.
[20] E. Deprez, M.A. Munoz-Marquez, M.A. Roldan, C. Prestipino, F.J. Palomares, C.B. Minella, U. Bösenberg, M. Dornheim, R. Bormann, A. Fernandez, J. Phys. Chem. C 114 (2010) 3309–3317.
[21] M.Q. Fan, L.X. Sun, Y. Zhang, F. Xu, J. Zhang, H.L. Chu, Int. J. Hydrogen Energy 33 (2008) 74–80.
[22] Y. Zhang, Q.F. Tian, H.L. Chu, J. Zhang, L.X. Sun, J.C. Sun, Z.S. Wen, J. Phys. Chem. C 113 (2009) 21964–21969.
[23] U. Bösenberg, U. Vainio, P.K. Pranzas, J.M. Bellosta von Colbe, G. Goerigk, E. Welter, M. Dornheim, A. Schreyer, R. Bormann, Nanotechnology 20 (2009) 1–9 (204003).
[24] P.J. Wang, Z.Z. Fang, L.P. Ma, X.D. Kang, P. Wang, Int. J. Hydrogen Energy 35 (2010) 3072–3075.
[25] U. Bösenberg, D.B. Ravnsbak, H. Hagemann, V. D'Anna, C.B. Minella, C. Pistidda, W. Beek, T.R. Jensen, R. Bormann, M. Dornheim, J. Phys. Chem. 114 (2010) 15212–15217.
[26] J.H. Shim, J.H. Lim, S. Rather, Y.S. Lee, D. Reed, Y.H. Kim, D. Book, Y.W. Cho, J. Phys. Chem. Lett. 1 (2010) 59–63.
[27] J.W. Christian, The Theory of Transformations in Metals and Alloys , 2nd edition, Pergamon, 2002.